Wilfried Elmenreich, J. Tenreiro Machado
and Imre J. Rudas (Eds)

Intelligent Systems

at the Service of Mankind

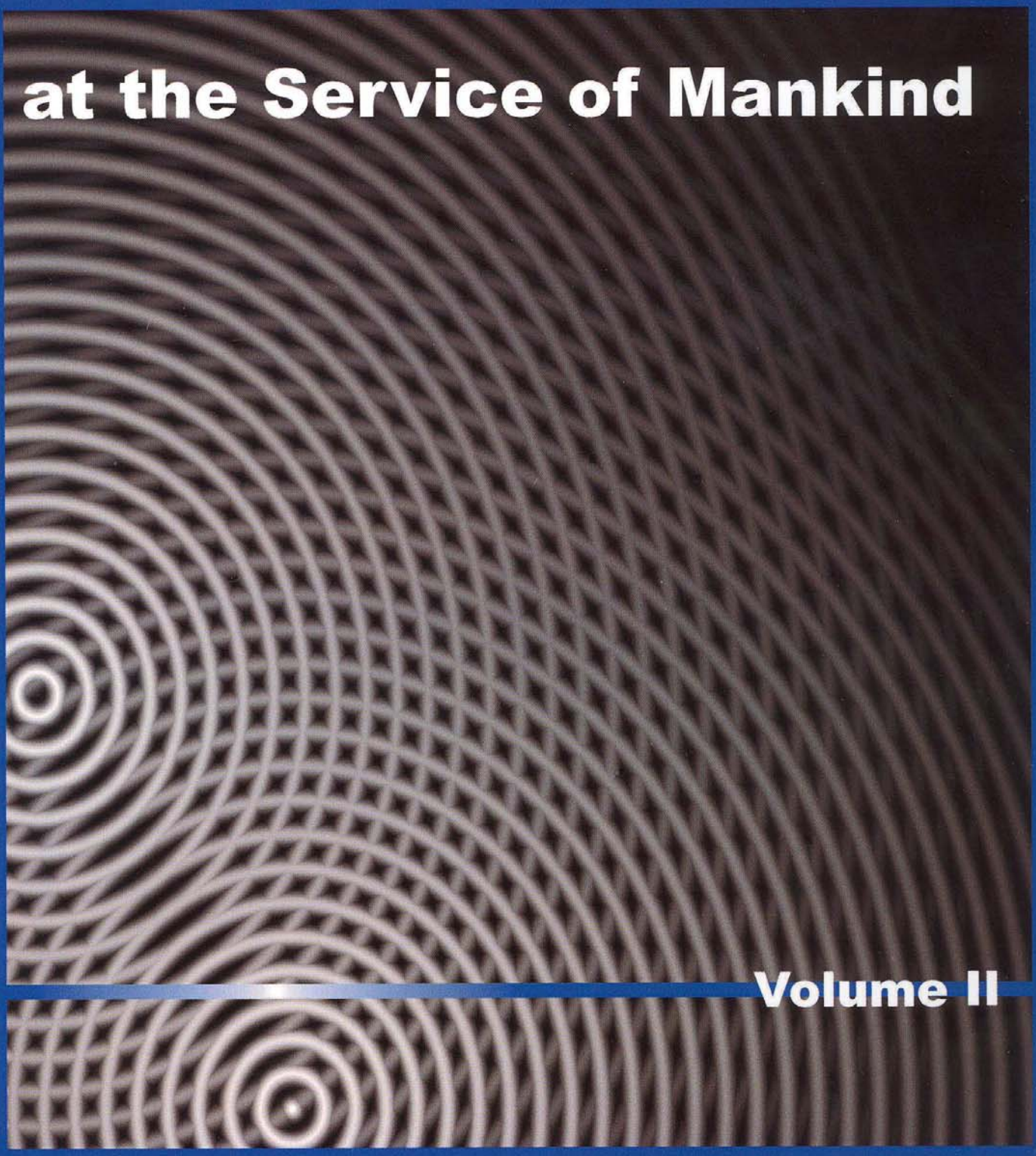

Volume II

Analysis of Two Arms Working in Cooperation

N. M. Fonseca Ferreira[1], J. A. Tenreiro Machado[2], and J. Boaventura Cunha[3]

[1]Dept. of Electrical Engineering,
Institute of Engineering of Coimbra, Rua Pedro Nunes, 3031-601 Coimbra, Portugal
nunomig@mail.isec.pt

[2]Dept. of Electrical Engineering,
Institute of Engineering of Porto, Rua Dr Ant. Bern. de Almeida, 4200-072 Porto, Portugal
jtm@isep.ipp.pt

[3]University of Trás-os-Montes e Alto Douro,
Ap 1013, 5000-911 Vila Real, Portugal
jboavent@utad.pt

Abstract — *This paper analyzes the performance of two cooperative robot manipulators. In order to capture the working performance we formulated several performance indices that measure the manipulability, the effort reduction and the equilibrium between the two robots. In this perspective the proposed indices we determined the optimal values for the system parameters. Furthermore, it is studied the implementation of fractional-order algorithms in the position/force control of two cooperating robotic manipulators holding an object.*

1 Introduction

Two robots carrying a common object are a logical alternative for the case in which a single robot is not able to handle the load. The choice of a robotic mechanism depends on the task or the type of work to be performed and, consequently, is determined by the position of the robots and by their dimensions and structure. In general, the selection is done through experience and intuition; nevertheless, it is important to measure the manipulation capability of the robotic system [1], that can be useful in the robot operation. In this perspective it was proposed the concept of kinematic manipulability measure [2] and its generalization dynamical manipulability [3] or, alternatively, to a statistical evaluation of manipulation [4]. Other related aspects such as the coordination of two robots handling objects, collision avoidance and free path planning have been also investigated [5, 6] but still require further study. Furthermore, with two cooperative robots the resulting interaction forces have to be accommodated and consequently, in addition to position feedback, force control is also required to accomplish adequate performances [7, 8, 9]. There are two basic methods for force control, namely the hybrid position/force and the impedance schemes. The first method [10] separates the task into two orthogonal sub-spaces cor-

responding to the force and the position controlled variables. Once established the subspace decomposition two independent controllers are designed. The second method [11] requires the definition of the arm mechanical impedance. The impedance accommodates the interaction forces that can be controlled to obtain an adequate response. This paper analyzes the manipulation and the payload capability of two arm systems. Through the formulation of several indices we analyze the robot actuator efforts and payload balance, and we study the position/force control of two cooperative manipulators, using fractional-order FO algorithms [12, 13, 14, 15]. Bearing these facts in mind this article is organized as follows. Section two, determines the manipulability of robotic systems, based on a numerical method and section three studies the performance of two-arm systems. Section four presents the controller architecture for the position/force control of two robotic arms and introduces the fundamentals of the fractional-order algorithms. Based on these concepts, we develop several experiments for the analysis and the performance evaluation of FO and the PID controllers, for robots having several types of dynamic phenomena at the joints. Finally, section five outlines the main conclusions.

2 The Manipulability of Robotic Systems

The manipulability measures the robot efficiency in the workspace from the viewpoint of object handling capability. For one arm the kinematic manipulability μ is defined as:

$$\mu = |det[J(q)J^T(q)]|^{1/2} \tag{1}$$

where J is Jacobian of the robot kinematics. With this formulation, for the RR robot it yields $\mu = l_1 l_2 |sinq_2|$ where l_i and q_i $(i = 1, 2)$ are the length and position of link i, respectively. Therefore, we verify that the best posture for the RR robot occurs when $q_2 = 90$. Besides, for a total length $l_1 + l_2 = L$, the manipulability μ has a maximum when $l_1 = l_2$. For one robot the analytical development of μ is straightforward; however, for two or more robots the definition of μ is more complex. To overcome this problem we adopt a numerical approach inspired by the Monte Carlo method. The method [7] consists in establishing a grid of m points in the workspace and, for each of these points, to generate a sample of n points in the interior of a sphere with a radius ρ in the joint space. Each point mapped into the operational space through the direct kinematics, in order to obtain the corresponding ellipsoid set of points. The size and shape of the ellipsoids determine the "amplification" between the joint space and the operational space and is related to eigenvalues of the kinematics Jacobian. The manipulability varies in the workspace. Therefore, we consider the index μ_{Av} that represents the average volume of μ in all the possible workspace W.

$$\mu_{Av} = Av[\mu(x, y), \forall (x, y) \in W] \tag{2}$$

The following experiments adopt one and two robots with RR structure. In a first phase we consider a single robot, in order to compare the analytical and numerical methods. In a second phase we consider two robots working in cooperation (figure 1) in order to determinate the manipulability of the total system and the system configuration that leads to a superior performance.

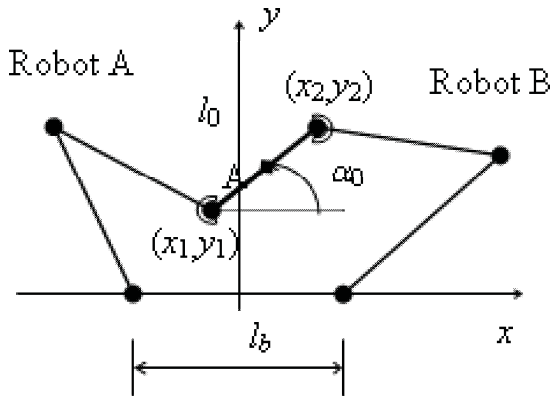

Figure 1: Two RR robots working in cooperation for the manipulation of an object with length l_0, orientation $\alpha_0$and distance l_b between the shoulders.

Figure 2 show the manipulability for one RR robot in the workspace obtained by the two alternative methods.

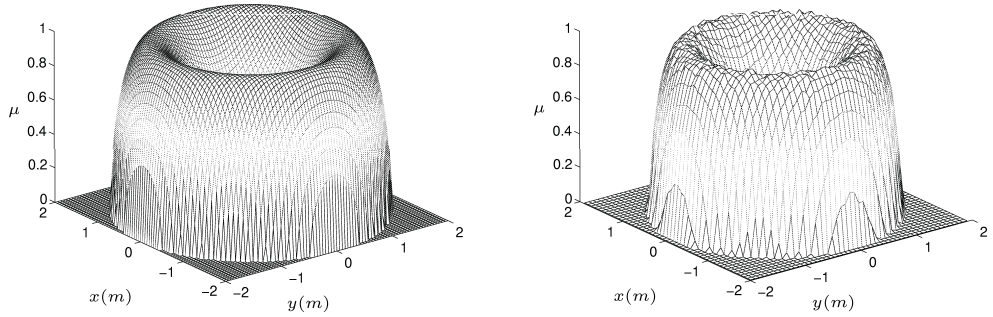

Figure 2: Manipulability μ of one RR robot with l_1 = 1 m and l_2 = 0.8 m obtained by the: a) analytical method, b) numerical algorithm for m = 1000 points, n = 1000 points, ρ = 0.1 *rad*.

As we can see, the numerical method presents a small error when compared with the analytical expression. Furthermore, the new algorithm has a low computational cost and it is easy to implement. Obviously, to decrease the numerical error it is necessary to increase the m and n, but the calculation time increases proportionally.

The figure 3 shows μ_{Av}as function of the distance l_b between the arm elbows and reveals that we obtain larger values for $l_b \approx 0$ with l_0 = 0 or l_b = 1 with l_0 = 1 because the workspace is maximum in that case, while the best case occurs for $l_1 = l_2$.

Another important aspect of robot cooperation is the manipulability variation within the system workspace. In this line of thought, we compare μ_{Av} for distinct robot object orientations α_0 and different sizes of the object l_0 and several distances l_b between the robot shoulders. In the experiments we consider $0 \leq l_b \leq l_1 + l_2 + l_0$, $l_0 = l_b = 1$ and $\alpha_0 = 0$.

Figure 4 and 5 show the indice μ_{Av} versus the parameters l_b, α_0 and l_0 for two cooperating RR robots. This numerical experiment considers a grid of m = 1000 points and, for each of these points, a sample of n = 1000 points, inside a sphere with a radius of ρ = 0.1 *rad* in the joint space.

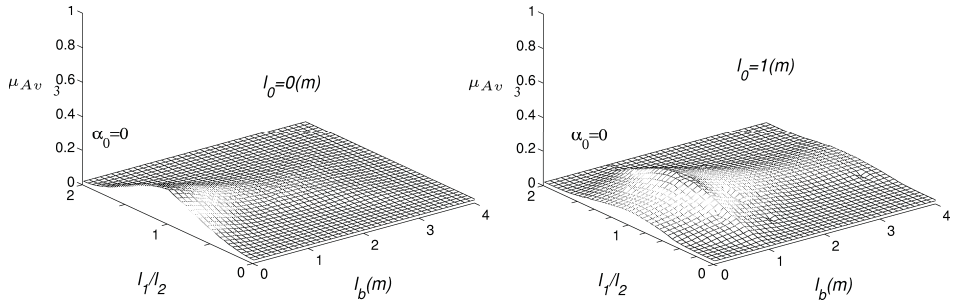

Figure 3: Average manipulability μ_{Av} in the workspace of two RR robots working in cooperation for $l_b \in [0, 4[$ *versus* l_1/l_2 with $l_1 + l_2$ = 2 m, l_0 = 0 m and l_0 = 1 m for α_0= 0^o.

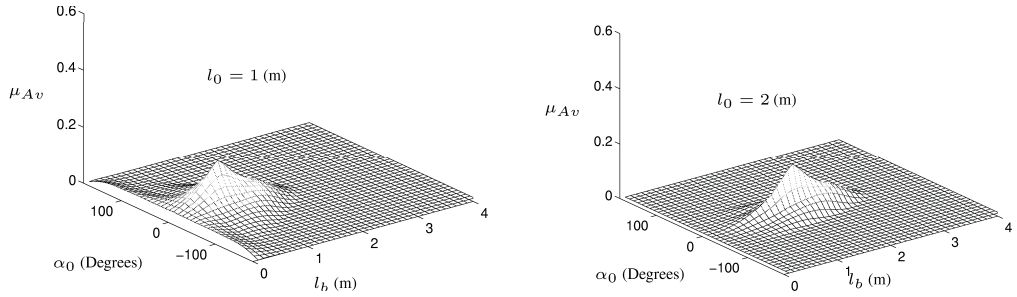

Figure 4: Two-arm average manipulability μ_{Av} *versus* l_b and α_0 for object lengths $l_0 = \{1, 2\}$, with m = 1000, n = 1000, $\rho =$ 0.1 and two RR robots with $l_1 = l_2$ = 1 m.

Figures 4 reveal that we get a maximum manipulability for α_0 = 0 and Figure 5 shows the best situation occurs $l_0 = l_b$.

3 Measures for performance evaluation

In this section it is analyzed the reduction of the joint actuator efforts and the payload equilibrium between the two cooperative robots. In mathematical terms we provide several global measures that compare the performance of one and two arm systems. In this line of thought the indices φ_1 and φ_2 measure the effort reduction and the indice φ_3 captures the equilibrium between the two arms:

$$\text{One robot} \qquad T^2 = T_1^2 + T_2^2 \tag{3a}$$

$$\text{Two robot} \qquad \left.\begin{array}{l} T_A^2 = T_{1A}^2 + T_{2A}^2 \\ T_B^2 = T_{1B}^2 + T_{2B}^2 \end{array}\right\} \Longrightarrow T_{AB}^2 = T_A^2 + T_B^2 \tag{3b}$$

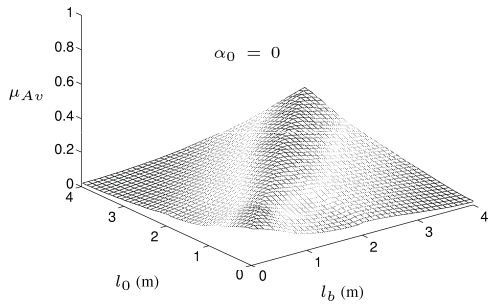

Figure 5: Two-arm average manipulability μ_{Av}*versus* l_0 and l_b for α_0 = 0, $l_0 \in$ [0, 4], $l_b \in$ [0, 4], m = 1000, n = 1000, $\rho =$ 0.1 and two RR robots with $l_1 = l_2$ = 1 m.

$$\varphi_1 = \sqrt{\frac{T_A^2}{T^2}} = \frac{|T_A|}{|T|} \tag{3c}$$

$$\varphi_2 = \sqrt{\frac{T_{AB}^2}{T^2}} = \frac{|T_{AB}|}{|T|} \tag{3d}$$

$$\varphi_3 = \sqrt{\frac{T_A^2}{T_{AB}^2}} = \frac{|T_A|}{|T_{AB}|} \tag{3e}$$

Figure 6 shows the relation between the maximal and minimal torques in all the workspace for one and two arm systems. We conclude that for a payload mass $M > 1kg$ we have |T| $>$ |T$_{AB}$| and for large payloads we get |T| $\approx$ 2.|T$_{AB}$|. The Figure 7 shows that for operating points near the singularities the two-arm systems presents same problems. Nevertheless, in the major part of the workspace we have a substantial reduction of the torque actuators.

Furthermore, the index φ_3 reveals a good equilibrium between the two arms independently of the payload.

4 Position Force Control of Two Arms

With two cooperative robots the resulting interaction forces have to be accommodated and consequently, in addition to position feedback, force control is also required. Therefore in order to get good performances it is necessary to specify no only the desired motion of each robot but also the corresponding handling force.

In the system under study the contact of the robot gripper with the load is modeled through a linear system with a mass M, a damping B and a stiffness K. On the other hand, the dynamics of a robot with n links interacting with the environment is modeled as:

$$\tau = \mathbf{C}(\mathbf{q}, \dot{\mathbf{q}}) + \mathbf{G}(\mathbf{q}) - \mathbf{J}^{\mathbf{T}}(\mathbf{q})\mathbf{F} + \mathbf{H}(\mathbf{q})\ddot{\mathbf{q}} \tag{4}$$

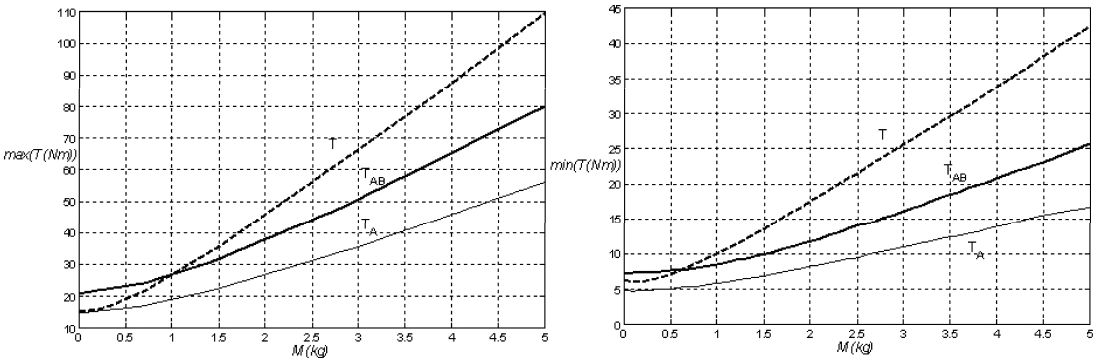

Figure 6: The maximal and minimal torques of one RR robot $|T|$, two RR robots $|T_{AB}|$ and left robot $|T_A|$ *versus* the payload mass M_0 with l_b = 1 m, α_0 = 0 and two RR robots with $l_1 = l_2$ = 1 m.

where τ is the $n \times 1$ vector of actuator torques, **q** is the $n \times 1$ vector of joint coordinates, **H(q)** is the $n \times n$ inertia matrix,$\mathbf{C}(\mathbf{q}, \dot{\mathbf{q}})$ is the $n \times 1$ vector of centrifugal / Coriolis terms and **G(q)** is the $n \times 1$ vector of gravitational effects. The matrix $\mathbf{J}^T$**(q)** is the transpose of the Jacobian and **F** is the force that the load exerts in the robot gripper.
We consider RR manipulators (n = 2) with dynamics:

$$\mathbf{C}\left(\mathbf{q}, \dot{\mathbf{q}}\right) = \begin{bmatrix} -m_2 r_1 r_2 S_2 \dot{q}_2^2 - 2 m_2 r_1 r_2 S_2 \dot{q}_1 \dot{q}_2 \\ m_2 r_1 r_2 S_2 \dot{q}_1^2 \end{bmatrix} \tag{5a}$$

$$\mathbf{G}\left(\mathbf{q}\right) = \begin{bmatrix} g\left(m_1 r_1 C_1 + m_2 r_1 C_1 + m_2 r_2 C_{12}\right) \\ g m_2 r_2 C_{12} \end{bmatrix} \tag{5b}$$

$$\mathbf{J^T}\left(\mathbf{q}\right) = \begin{bmatrix} -r_1 S_1 - r_2 S_{12} & r_1 C_{11} + r_2 C_{12} \\ -r_2 S_{12} & r_2 C_{12} \end{bmatrix} \tag{5c}$$

$$\mathbf{H}\left(\mathbf{q}\right) = \begin{bmatrix} (m_1 + m_2) r_1^2 - m_2 r_2^2 + 2 m_2 r_1 r_2 C_2 + J_{1m} + J_{1g} & m_2 r_2^2 + m_2 r_1 r_2 C_2 \\ -m_2 r_2^2 + m_2 r_1 r_2 C_2 & m_2 r_2^2 + J_{2m} + J_{2g} \end{bmatrix} \tag{5d}$$

where C_{ij} = cos(q_i + q_j) and S_{ij} = sin(q_i + q_j).

To simplify we consider both robots with identical dimensions and the contact of the robot gripper with the load is modeled through a linear system with a mass M, a damping B and a stiffness K. The numerical values adopted for the RR robots and the object are m_1 = m_2 = 1.0 kg l_1 = l_2 = l_b = l_0 = 1.0 m, α_0 = 0 deg, B_1 = B_2 = 1 Ns.m^{-1} and K_1 = K_2 = 10^4 Nm^{-1}.

The controller architecture (Figure 8) is inspired on the impedance and compliance schemes. Therefore, we establish a cascade of force and position algorithms as internal

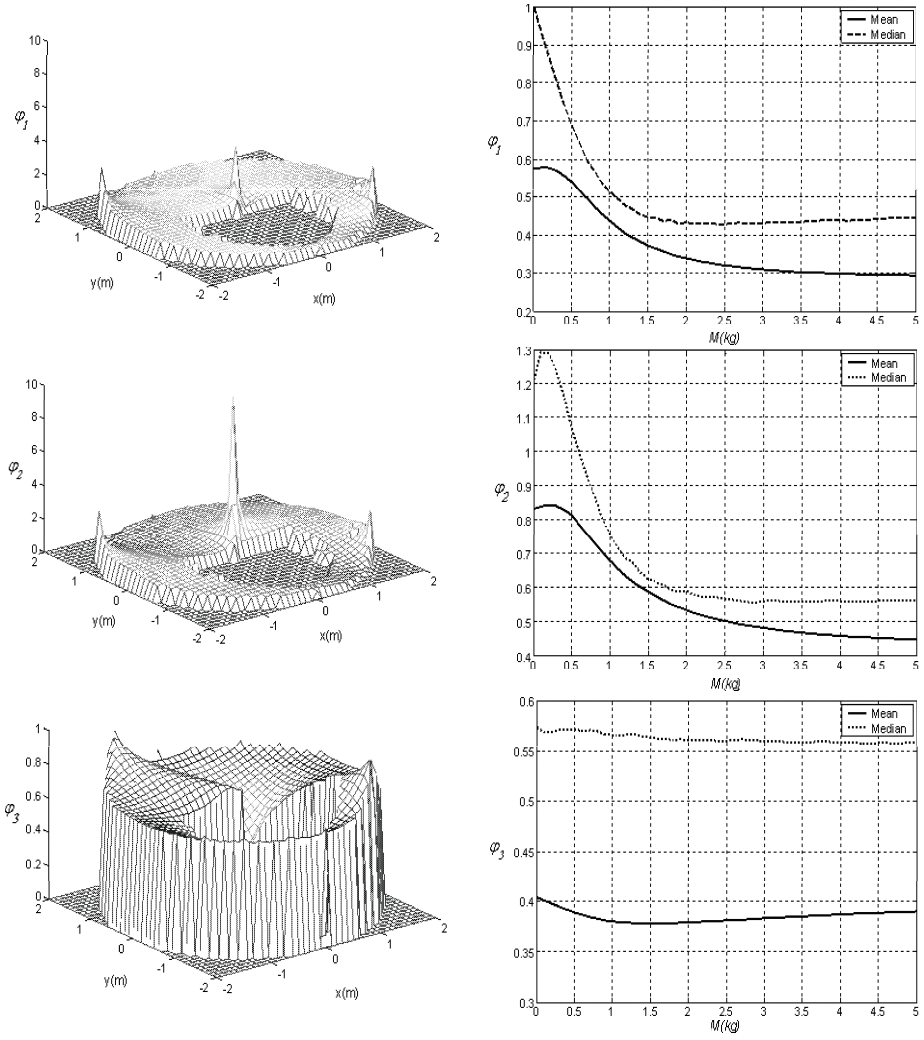

Figure 7: The maximal and minimal torques of one RR robot $|T|$, two RR robots $|T_{AB}|$ and left robot $|T_A|$ *versus* the payload mass M_0 with l_b = 1 m, α_0 = 0 and two RR robots with $l_1 = l_2$ = 1 m.

an external feedback loops, respectively, where $\boldsymbol{x}_d$ and $\boldsymbol{F}_d$ are the payload desired position coordinates and contact forces.

In the position and force control loops we consider FO controllers. The mathematical definition of a derivative of fractional order α has been the subject of several different approaches. For example, we can mention the Laplace and the Grünwald-Letnikov definitions:

$$D^{\alpha}[x(t)] = \mathcal{L}^{-1}\{s^{\alpha}X(s)\} \tag{6}$$

$$D^{\alpha}\left[x\left(t\right)\right] = \lim_{h\to 0}\left[\frac{1}{h^{\alpha}}\sum_{k=1}^{\infty}\frac{\left(-1\right)^{k}\Gamma\left(\alpha+1\right)}{\Gamma\left(k+1\right)\Gamma\left(\alpha-k+1\right)}x\left(t-kh\right)\right] \tag{7}$$

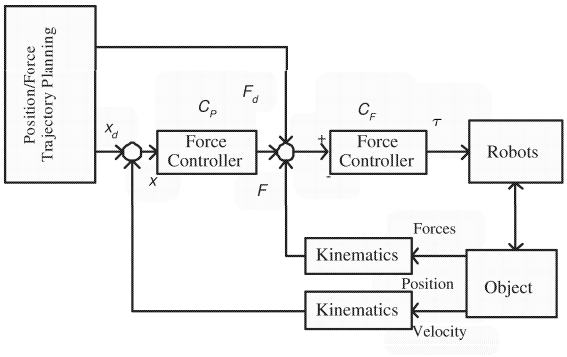

Figure 8: The position/force cascade controller.

where Γ is the gamma function and h is the time increment.
In our case, for implementing FO algorithms of the type $C(s) = K_p + K\, s^{\alpha}$, $-1 < \alpha < 1$, we adopt a 4^{th}-order discrete-time Pade approximation ($a_i,\ b_i,\ c_i,\ d_i \in \mathbb{R}$, $k = 4$):

$$C_P(z) \approx K_P \frac{a_0 z^k + a_1 z^{k-1} + .. + a_k}{b_0 z^k + b_1 z^{k-1} + ... + b_k} \tag{8a}$$

$$C_F(z) \approx K_F \frac{c_0 z^k + c_1 z^{k-1} + .. + c_k}{d_0 z^k + d_1 z^{k-1} + ... + d_k} \tag{8b}$$

To analyze the system performance we consider both robots with ideal transmissions and robots with dynamic phenomena at the joints, such as backlash. Moreover, we compare the response of *FO* and classical algorithms namely PD: $C_P(s) = K_p\ (1 + T_d s)$ and PI: $C_F(s) = K_F\ [1 + \frac{1}{T_i s}]$, in the position and force loops, respectively.

Both algorithms were tuned by trial and error having in mind getting a similar performance in the two cases. The resulting parameters were *FO*: $\{K_P$,$\alpha_P\} \equiv \{10^4,\ 1/2\}$, $\{K_F\ ,\alpha_F\} \equiv \{2, 1/5\}$ and $PD - PI$: $\{K_p$,$K_d\} \equiv \{10^4$,$10^2\}$, $\{K_p$,$K_i\} \equiv \{10$,$10^4\}$ for the position and force loops, respectively. In order to study the system dynamics we apply, separately, small amplitude rectangular pulses, at the position and force references, that is, we perturb the references with: $\{\delta x_d, \delta y_d, \delta Fx_d, \delta Fy_d\} = \{10^{-3}, 0, 0, 0\}$, $\{\delta x_d, \delta y_d, \delta F_d, \delta Fy_d\}$ $=\{0, 10^{-3}, 0, 0\}$,$\{\delta x_d, \delta y_d, \delta Fx_d, \delta Fy_d\} = \{0, 0, 1, 0\}$, $\{\delta x_d, \delta y_d, \delta Fx_d, \delta Fy_d\} = \{0, 0, 0, 1\}$.

Furthermore, in order to evaluate the robustness of the *FO* algorithms, we compare the response for robots with dynamical phenomena at the joints. In all experiments controller sampling frequency f_c = 10 kHz, contact forces of the grippers $\{Fx_j$,$Fy_j\} \equiv \{0.5$,$5\}$ *Nm* (j = A, B) operating point at the center of the object A$\equiv\{x$,$y\} \equiv \{0$,$1\}$ and $\theta = 0^o$.

In a first phase we consider robots with ideal transmissions at the joints. Figures 9 and 10 depict the time response of robot A under the action of the FO and $PD - PI$ algorithms.

In a second phase (Figure 11) we analyze the response of robots with dynamic backlash at the joints. For the ith joint gear (i= 1, 2), with clearance h_i, the backlash reveals impact phenomena between the inertias, which obey the principle of conservation of momentum and the Newton law:

$$\dot{q}_i' = \frac{\dot{q}_i \left(J_{ii} - \varepsilon J_{im}\right) + \dot{q}_{im} J_{im} \left(1 + \varepsilon\right)}{J_{ii} + J_{im}} \tag{9a}$$

$$\dot{q}_{im}' = \frac{\dot{q}_i J_i \left(1 + \varepsilon\right) + \dot{q}_{im} \left(J_{im} - \varepsilon J_{ii}\right)}{J_{ii} + J_{im}} \tag{9b}$$

where $0 \leq \varepsilon \leq 1$ is a constant that defines the type of impact (ε = 0 inelastic impact, ε = 1 elastic impact) and $\dot{q}_i'$ and $\dot{q}_{im}'$ are the inertias velocities of the ith joint and motor after the collision, respectively. The parameter J_{ii} (J_{im}) stands for the link (motor) inertias of joint i. The numerical values adopted are h_i = 1.8 10^{-4} rad and ε_i = 0.8.

The time responses characteristics (Tables I, II, III and IV), namely the percent overshoot $PO\%$, the steady-state error e_{ss}, the peak time T_p and the settling time T_s, reveal that, although tuned for similar performances in the first case, the FO is superior to the $PD - PI$ particularly in the cases with dynamical phenomena at the robot joints.

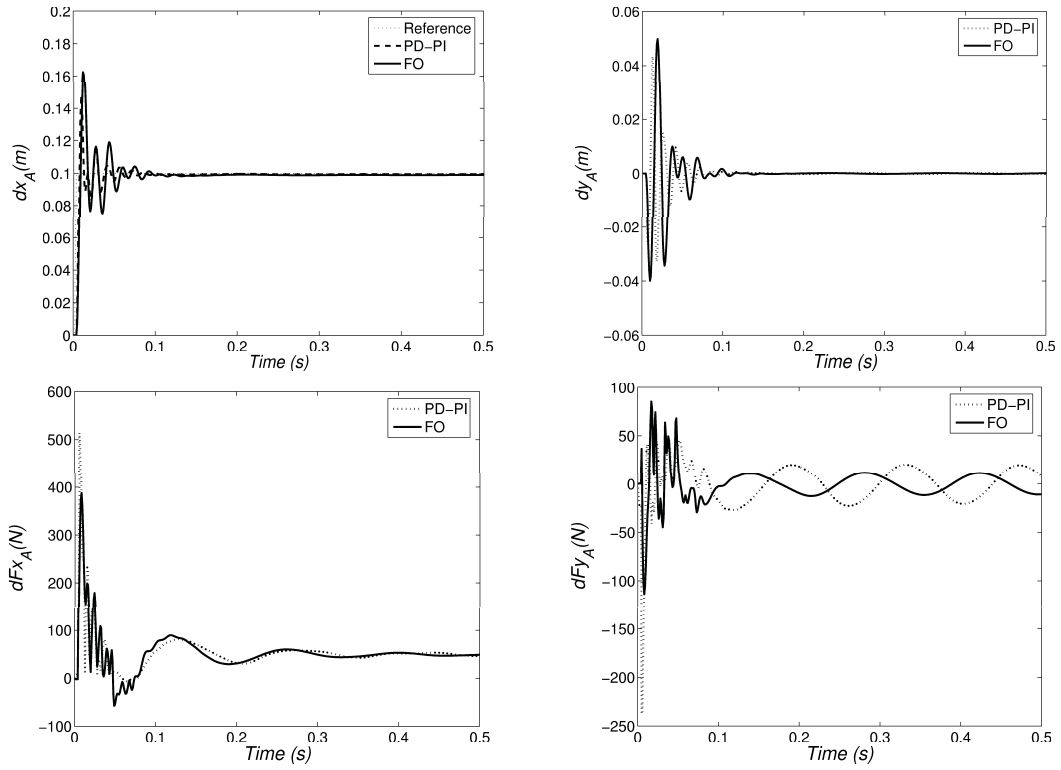

Figure 9: Time response for robots with ideal joints under the action of the FO and $PD - PI$ algorithms for a reference position perturbation δy_d = 0.1 m and a payload with the parameters of M_0 = 1 kg, B_i = 10 Ns/m and K_i = 10^3 N/m.

5 Conclusions

This paper studied of the manipulation capability of two robots working in cooperation. In this perspective, a numerical tool was introduced for the analysis of the manipulability of

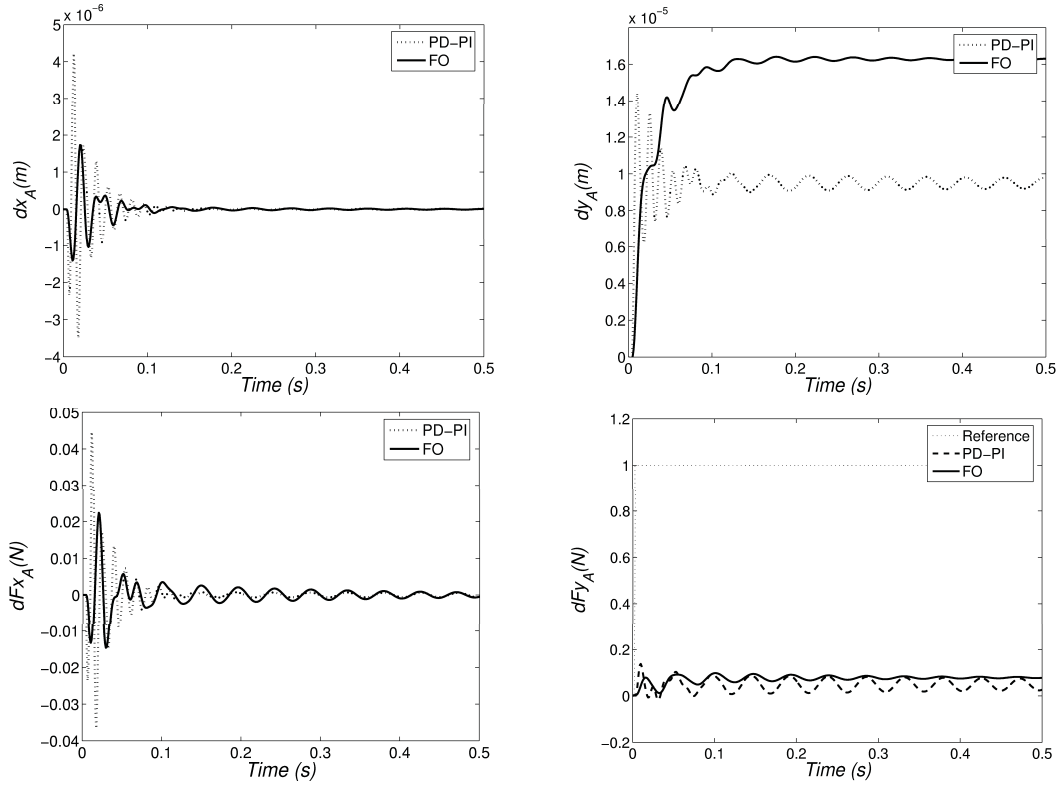

Figure 10: Time response for robots with ideal joints under the action of the FO and $PD - PI$ algorithms for a reference force perturbation δFy_d = 1 N and a payload with the parameters of M_0 = 1 kg, B_i = 10 Ns/m and K_i = 10^3 N/m.

Table 1: Time response for a pulse δx_d the robot A position reference.

Joint		*PO%*	e_{ss}	T_p	T_s
ideal	*PID*	59.98	1.4 10^{-4}	1 10^{-3}	22 10^{-2}
	FO	54.81	1.3 10^{-4}	1 10^{-3}	12 10^{-2}
backlash	*PID*	4.05	1.0 10^{-3}	5 10^{-2}	10 10^{-2}
	FO	1.0	1.3 10^{-4}	25 10^{-2}	30 10^{-2}

Table 2: Time response for a pulse δy_d the robot A position reference.

Joint		*PO%*	e_{ss}	T_p	T_s
ideal	*PID*	59.0	1.5 10^{-4}	1 10^{-3}	22 10^{-2}
	FO	54.31	1.3 10^{-4}	1 10^{-3}	12 10^{-2}
backlash	*PID*	3.05	1.2 10^{-3}	5 10^{-2}	10 10^{-2}
	FO	1.2	1.3 10^{-4}	25 10^{-2}	30 10^{-2}

Table 3: Time response for a pulse δFx_d at the robot A force reference.

Joint		*PO%*	e_{ss}	T_p	T_s
ideal	*PID*	52.58	95 10^{-2}	54 10^{-5}	99 10^{-2}
	FO	8.14	90 10^{-2}	41 10^{-5}	25 10^{-3}
backlash	*PID*	20.12	93 10^{-2}	50 10^{-2}	50 10^{-2}
	FO	12.4	90 10^{-2}	27 10^{-2}	50 10^{-2}

Table 4: Time response for a pulse δFy_d at the robot A force reference.

Joint		*PO%*	e_{ss}	T_p	T_s
ideal	*PID*	52.50	95 10^{-2}	55 10^{-5}	99 10^{-2}
	FO	8.12	90 10^{-2}	40 10^{-5}	25 10^{-3}
backlash	*PID*	20.14	93 10^{-2}	48 10^{-2}	86 10^{-2}
	FO	11.81	90 10^{-2}	55 10^{-2}	60 10^{-2}

multiple robots in the workspace. Based on the new algorithm it was possible to compare distinct situations, such as different sizes and orientations of the object and distinct lengths between the two arms. Moreover, were also evaluated the actuator joint efforts and the payload distribution. In a second part of the paper it was studied the position/force control

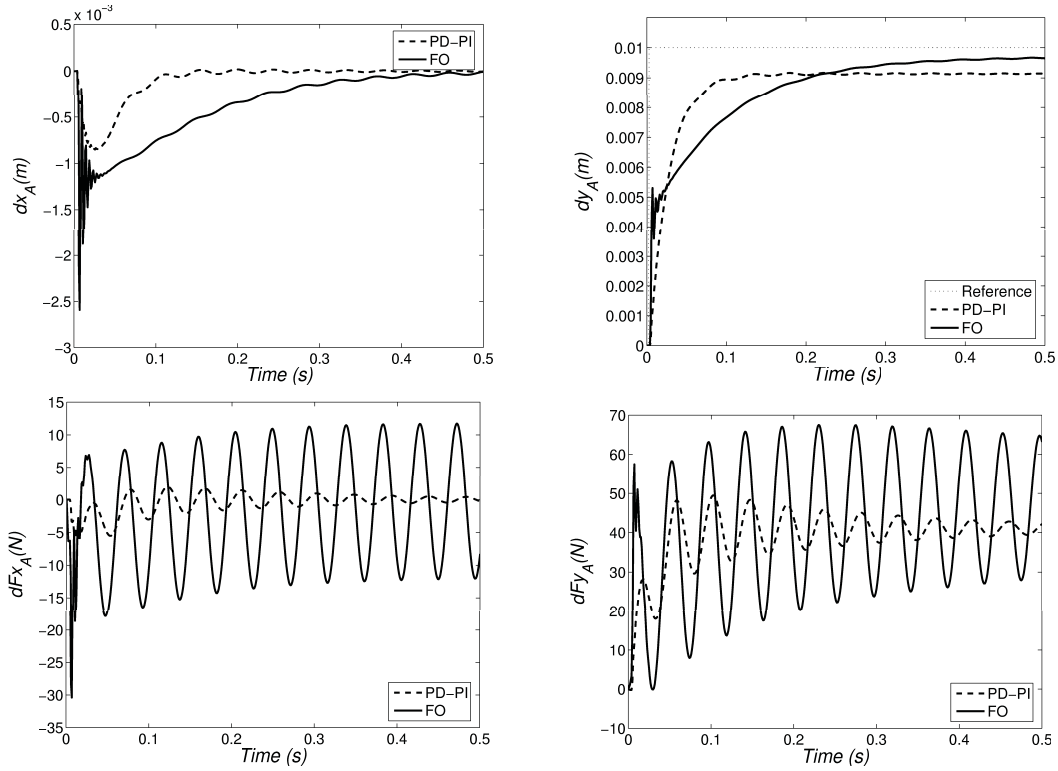

Figure 11: Time response for robots with joints having backlash under the action of the FO and $PD - PI$ algorithms for a pulse perturbation at the robot A position reference δy_d = 10^{-3}m and a payload with the parameters M_0 = 1 kg, B_i = 1 Ns/m and K_i = 10^3 N/m.

of two robots working in cooperation using fractional order and classical integer order control algorithms. The system dynamic performance was analyzed for manipulators having several types of dynamical phenomena at the joints. The results demonstrated that the fractional-order algorithm reveals a good performance and a high robustness.

References

[1] Y. C. Tsai and A.H Soni. Accessible region and synthesis of robot arms. *ASME J. Mech. Design, vol. 103*, pages 803–811, 1981.

[2] T. Yoshikawa. Manipulability of robotic mechanisms. *The Int. J. Robotics Research, vol. 4*, pages 3–9, 1985.

[3] H. Asada. A geometrical representation of manipulator dynamics and its application to arm design. *ASME J. Dynamic Syst. Meas., Contr., vol. 105*, pages 131–142, 1983.

[4] J. A. T. Machado and A. M. Galhano. A statistical and harmonic model for robot manipulators. *IEEE Int. Conf. on Robotics and Automation, Albuquerque, New Mexico, USA*, 1997.

[5] T. Yoshikawa Y. Nakamura, K. Nagai. Dynamics and stability in coordination of multiple robotic mechanisms. *International Journal of Robotics Research, vol. 8*, pages 44–61, 1989.

[6] P. K. De T. J. Tarn, A. K. Bejczy. Analysis of the dynamic ability of two robot arms in object handling. *Advanced Robotics, vol. 10, n. 3*, pages 301–315, 1996.

[7] J. A. Tenreiro Machado N. M. Fonseca Ferreira. Manipulability analysis of two-arm robotic systems. *4th IEEE International Conference on Intelligent Engineering Systems, Portoroz, Slovenia*, 2000.

[8] A. K. Bejczy and T. Jonhg Tarn. Redundancy in robotics connected robots arms as redundant systems. *4th IEEE International Conference on Intelligent Engineering Systems, Portoroz, Slovenia*, 2000.

[9] M. H. Raibert and J. J. Craig. Hybrid position/force control of manipulators. *ASME J. of Dynamic Systems, Measurement and Control, vol. 2, n. 2*, pages 126–133, 1981.

[10] J. Boaventura Cunha N. M. Fonseca Ferreira, J. A. Tenreiro Machado. Fractional-order position/force robot control. *2nd IEEE Int. Conference on Computational Cybernetics, Vienna, Austria*, pages 126–133, 2004.

[11] N. Hogan. Impedance control: An approach to manipulation, parts i-theory, ii-implementation, iii-applications. *ASME J. of Dynamic Systems, Measurement and Control, vol. 107, No. 1*, pages 1–24, 1985.

[12] N. M. Fonseca Ferreira and J. A. Tenreiro Machado. Fractional-order hybrid control of robotic manipulator. *11th IEEE Int. Conf. on Advanced Robotics, Coimbra, Portugal*, pages 1–24, 2003.

[13] A. Oustaloup. La drivation non entire: Thorie, synthse et applications. *Hermes, Paris*, pages 1–24, 1995.

[14] J. Tenreiro Machado. Analysis and design of fractional-order digital control systems. *J. Systems Analysis, Modelling and Simulation, vol. 27*, pages 107–122, 1997.

[15] I. Podlubny. Fractional-order systems and pi d -controllers. *IEEE Trans. on Automatic Control, vol. 44, no. 1*, pages 208–213, 1999.

About the Authors

Nuno Miguel Fonseca Ferreira was born in 1972. He graduated with a B.A. degree in the Institute of Engineering of the Polytechnic Institute of Coimbra, in 1994, and a degree in of Electrical engineering at the University of Porto, in 1996 and obtaining in 1999 the Master's degree in of Electrical and Computer Engineering. Presently he is Professor at the Institute of Engineering, Polytechnic Institute of Coimbra, and Department of Electrical Engineering. His main research interests are robotics and nonlinear systems.

J.A. T. Machado was born in 1957. He graduated and received the PhD degree in electrical and computer engineering from the Faculty of Engineering of the University of Porto, Portugal, in 1980 and 1989, respectively. Presently he is Coordinator Professor at the Institute of Engineering of Politecnic Institute of Porto, Department of Electrical Engineering. His main research interests are robotics, modeling, control, genetic algorithms, fractional-order systems and intelligent transportation systems.

José Boaventura Ribeiro da Cunha was born in 1961. Degrees: Electronics and Telecommunications Engineering (1985) at the University of Aveiro, Msc (1992), PhD (2002) degrees in Electrical Engineering at the University of TrásosMontes e Alto Douro, Portugal. Presently he is an Assistant Professor at the Engineering Department of the University of Trás-os-Montes e Alto Douro and he is a researcher at the CETAV Institute. His main research interests are automation and control systems.